COUPON Jean
Master 2 Recherche
Astrophysique et Astronomie

Université Pierre et Marie Curie (Paris VI)
Année 2005-2006

The Transit Timing method : how to detect extrasolar planets?

Supervisor: Norman W. Murray.

Master 2 final project. April 1st – June 30th 2006.
Canadian Institute for Theoretical Astrophysics

Contents

Introduction

The study of extrasolar planets leads us to a new way to learn about our own solar system and the mechanism of planet formation. The first planet was discovered in 1995, since then astrophysicists have been trying to improve the methods of detection. The three methods currently used are :

Radial velocities: This first one involves the motion of the star. The parameters of the planet are estimated from radial velocities measurements of the star such as orbital elements and mass. Planets in this case must have a Jupiter-like mass (down to 10 Earth masses for planets orbiting low mass stars). There is a degeneracy between inclination and mass (the amplitude of the effect depends on $M \sin i$).

Gravitational microlensing: The luminosity of the star is influenced by the relativistic effect of the planet's mass. The method can detect Earth-mass planets, however most orbital parameters will be uncertain.

Transits: When the planet passes in front of the star it reduces its brightness. The study of the light curve gives us a lot of information on the orbital parameters. The planet to star mass ratio is known with a very accurate value. But inclination must be small, therefore most of the systems cannot be detected by the transit method.

When there is only one planet, intervals between transits are exactly equal to the period of the planet. However the presence of other planets induces variations in the transit timings even though the perturbing planets do not transit. Matthew J. Holman and Norman W. Murray (2004) showed it was possible to use the transit timings to detect other planets in planetary systems. Space-based missions like Kepler will find transiting planets in the future and we can expect to discover many multiple planet systems.

In this project we focused on the transit method and the way to use it to detect other planets.
I worked with Norman Murray and Yanqin Wu at the Canadian Institute for Theoretical Astrophysics and the aim of my work was:

How to find the parameters of a second planet which perturbs a transiting planet?

We tried to answer the question by inverting the problem, given a set of transit timings.

- The first part of the report describes the transit phenomenon and how a perturbing planet affects this latter. Several cases will be showed.
- We propose in the second part a method to inverse the problem with the χ^2 minimization.

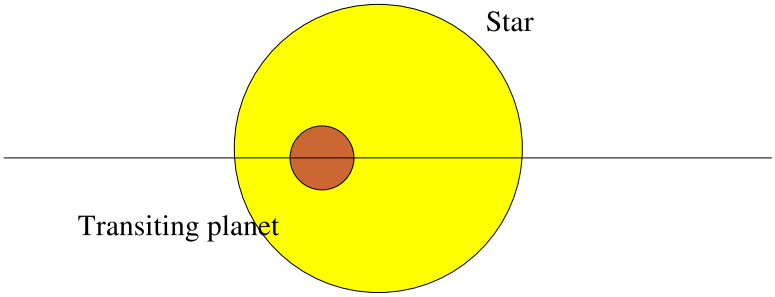

Figure 1: One single planet orbiting a star

Part I
Method and Numerical Calculations

In this part, we will look at the way to compute transit timings. The order of the effect is small compared to the planet period and we have to pay attention of how we do computations because it matters a lot. Let's recall that we are trying to invert the problem and at the end extract orbital parameters with the best possible accuracy. Because of degenerecies, different sets of parameters can be found given a same set of data as we will see in the next part. Therefore I chose to insist on the assumptions we are going to do.

The first section explains how to characterize a transit timing. It also shows the assumptions we made and introduces the causes of variations in the timings.

Then I will develop numerical aspects because it represents an important part of my work. I tried two ways to compute timings and I compare them in a last subsection.

Knowing what we learnt in the first two sections, we can finally analyse the effects of a perturbing planet on a transiting one.

1 The use of transit timing to detect extrasolar planets

1.1 Description of the system

The basic system is composed with a star and a transiting planet on a keplerian orbit (Figure 1). The transit occurs when both the planet and the star are aligned with the line of sight. If the system has only one planet, the time between two transits is constant and equals the orbital period, i.e.:

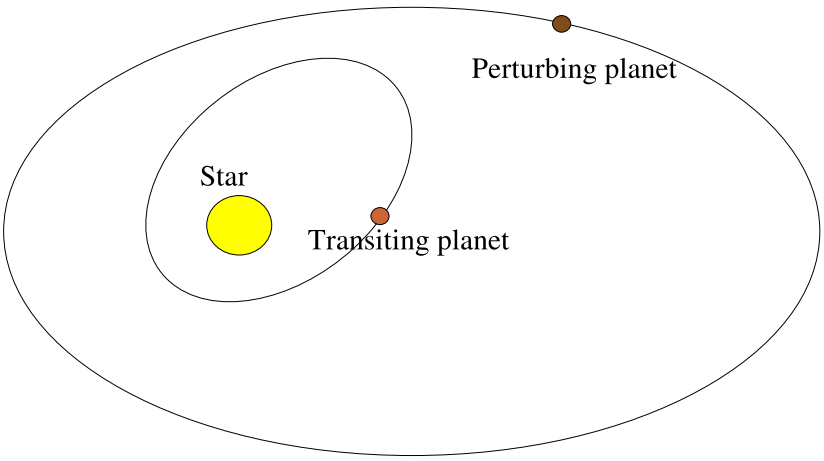

Figure 2: Both planets orbiting a star

$$\Delta t = t_{n+1} - t_n = T_1 \tag{1}$$

with

$$T_1 = \sqrt{\frac{4\pi^2}{\mu_1} a_1^3} \qquad \mu_1 = \mathcal{G}(M_\star + m_1) \tag{2}$$

and a_1 the planet semi-major axis.

The system we are interrested in has two planets orbiting a star (Figure 2). Because of the gravitational interactions, intervals between transits are not constant anymore:

$$\Delta t(t) = t_{n+1} - t_n = T_1 + \delta t(t) \tag{3}$$

We will call $\Delta t(t)$, the transit timing interval (between transits $n+1$ and n) and $\delta t(t)$, the transit timing variation.

We aslo define T_2, the period of the second planet:

$$T_2 = \sqrt{\frac{4\pi^2}{\mu_2} a_2^3} \qquad \mu_2 = \mathcal{G}(M_\star + m_2) \tag{4}$$

Throughout the rest of the report, “1” will characterize the transiting planet and “2” the perturbing planet.

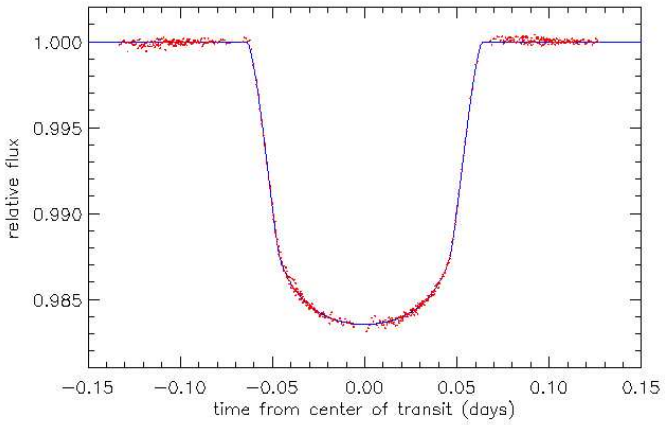

Figure 3: HD209458 transit (HST). Charbonneau et al.

1.2 Assumptions

We must make assumptions to render the study easier. General ones are the followings.

1. The transit timing is counted at the center of the transit (Figure 3).
2. The perturbing planet is an outer planet.
3. There are only two planets (spherical).
4. We consider an edge-on system (coplanar orbits). This is a good assumption for the transiting planet since we must see it, we will discuss it for the companion later.
5. The general relativity and tidal effects are neglected.
6. The center of mass has no external forces. We also neglect light travel time and parallax effects.
7. Transiting planets will be discovered by space-based missions but observations will be completed by ground-based telescopes. Then we assume a 5 to 10 second gaussian noise.
8. The star is a solar-mass star

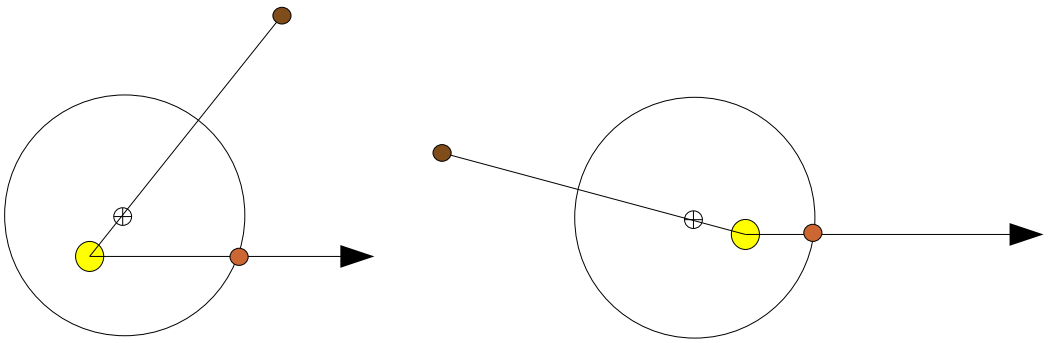

Figure 4: Left: transit at $t_0 = 0$, right: transit at $t_1 = T_1 + \delta t$

9. The transiting planet is a HD209458b-type planet with the parameters :
   Mass = $10^{-3} M_\star$
   T_1 = 3.52 days
   $a_1 = 4.5 \times 10^{-2} AU$
   e_1 = 0.025
   $i = 90^\circ$
   Longitude of ascending node = 0
   Argument of periapse = 0
   Mean anomaly (at $t = 0$) = 0
10. The observation time is about 2 years (170 transits)

Some of these assumptions will be discussed later...

1.3 The motion of the transiting planet trough the line of sight

This is an important point because even if the planets don't interact with each other (both of them on keplerian orbits) the transit intervals are different from the period of the transiting planet.

We look at motions in a barycentric frame. The perturbing planet is an outer planet. Let's assume for this subsection that the perturbing planet orbits the star on a keplerian orbit and the transiting planet orbits the star-perturbing planet barycentre.

As shown in figure 4, the wobble of the star due to the outer planet implies a late (or early) transit.

1.4 Direct and indirect effects of the perturbing planet

We now include the effects of the perturbing planet on the transiting one and we divide them into two.

The direct effect: is produced by the perturbing planet itself.

The indirect effect: is produced by the motion of the star induced by the perturbing planet.

The indirect effect reduces the amplitude of the effect described in subsection 1.3 because the wobble of the star tends to modify the orbit of the first planet (which "follows" the star).

However the orbit is not keplerian anymore and variations remain.

The variations in the transit timings are the sum of three effects:

- Transit must occur trough the line of sight.
- The second planet perturbs the motion by direct interactions.
- The motion of the star induced an indirect effect.

An other point of view is to consider motions in a heliocentric frame. Then the motion of the first planet can be seen as an orbit in a non-gallilean frame and perturbated by a second planet on a keplerian orbit.

2 Computation of transit timings

2.1 N-body simulation

The first step of this project was the numerical computation of the transit timings. I used a N-body code from M. Holman and N. Murray.

This code integrates the equations of motion in a Hamiltonian formulation, using a Leap-Frog integration algorithm. Energy in this case is very well conserved.

Motions are computed in the heliocentric frame, then the condition of transit was basically when the planet crosses the X-axis with a positive X-coordinate (see figure 5):

$$Transit \Leftrightarrow \begin{cases} y_{planet} = 0 \\ x_{planet} > 0 \end{cases} \tag{5}$$

Computing timings with an accuracy on the order of a second, takes a long time.To compute the transit timings in a reasonable time, the idea was to determine that a transit occured when the sign of the Y-coordinate changed, to go back and decrease the time interval of integration. The final difficulty is to reset position and velocity in the same point (since the Leap Frog integrator does not integrate those quantities in the same time).

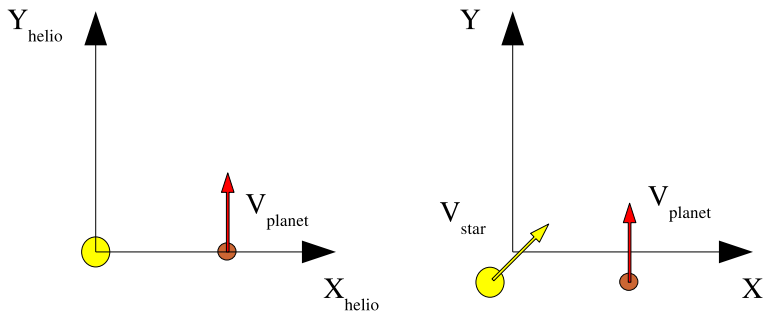

Figure 5: Left: transit computed in an heliocentric frame, right: in a barycentric frame

2.2 Bulirsch Stoer integrator

I wrote a code with the Bulirsch Stoer integration algorithm inspired again by a code from M. Holman and N. Murray. The code evaluates the position and the velocity at the same instant. This time, equations are integrated in a barycentric frame. The condition of transit becomes when the positions of the star and the inner planet are aligned (see figure 5):

$$Transit \Leftrightarrow \begin{cases} y_{planet} - y_{star} = 0 \\ x_{planet} > 0 \end{cases} \tag{6}$$

For a given integration time step, the algorithm extrapolates the function with many substeps until convergence is achieved (i.e. until errors estimates are small enough).

This way to compute the planet motions is very accurate but slow. However, as written above, positions and velocities are evaluated at the same instant and this allows us more flexibility.

Since the integrator converges towards a very accurate value for any given time step, I use an iterative method to find the timing transit. Imagine that we are looking for the root of the $y_{planet} - y_{star}$ function, search for transit timing can be accomplished by a simple dichotomic algorithm.

2.3 Comparisons

In order to display the results, we plot the time between two transits: $\Delta t(t) = t_{n+1} - t_n = T_1 + \delta t(t)$. Then we calculate the mean (which is close to T_1) and subtract it to each point.

Both codes give the same result (see figure 6 and 7). With the same accuracy ($1.10^{-5} days = 0.1 sec$):

- The N body code takes 1 min and 35 sec.

- The Bulirsch Stoer one takes only 3 sec.

We will obviously use the latter for our numerical computations. Nevertheless, the N-body code will be useful to check the long-term stability of the system.

3 Numerical results

3.1 Parameters dependencies

First we want to know what is the amplitude of the phenomenon. This first analysis will give us a set of constraints which will be detailed in the next part (Problem inversion).

To understand what is the effect of each parameter on the amplitude, we need to compute a large number of transits and record the extremum for each set of parameters. Then we plot the absolute value of the extremum with respect to the changing parameter, keeping the others constant.

We assumed we know the orbital parameters of the transiting planet, its mass and also assumed coplanar orbits. Therefore we want to know the parameters of the perturbing planet:

- Mass, m_2.
- Semi-major axis, a_2.
- Eccentricity, e_2.
- Argument of periapse, ϖ_2.
- Mean anomaly (at t = 0), M_2.

Mass: the bigger is the perturbing planet, the bigger is the amplitude of the effect. Thus we can immediately say that the amplitude of timing variations is a monotone function of the perturbing planet mass (figure 8).

Semi-major axis: as well as the mass, the closer is the second planet, the bigger is the effect. However we must take into account resonances which tend to increase significantly the effect. Near resonances ($\frac{T_2}{T_1} = n$), as expected, amplitude increases or decreases strongly (see figure 9).

Mean anomaly: an other immediate parameter dependency concerns the mean anomaly at $t = 0$. Since we are dealing with more than one hundred transits, we calculate transit timings during several periods of the second planet. The mean anomaly at $t = 0$ will not change the maximum of the variation.

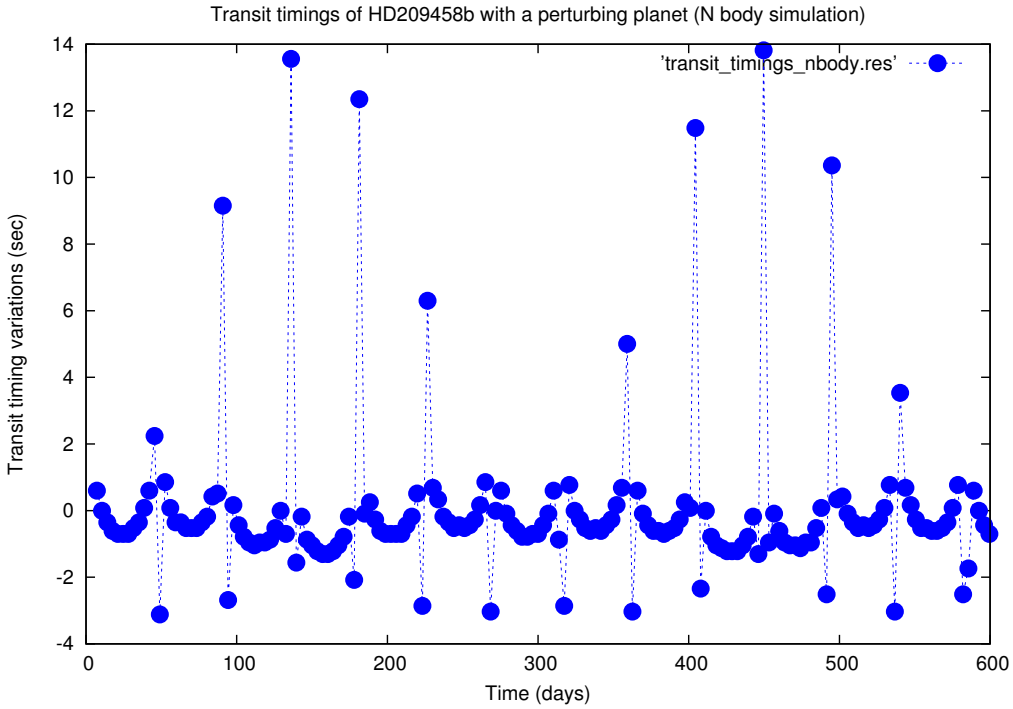

Figure 6: Transit timings computed with the N body simulation.

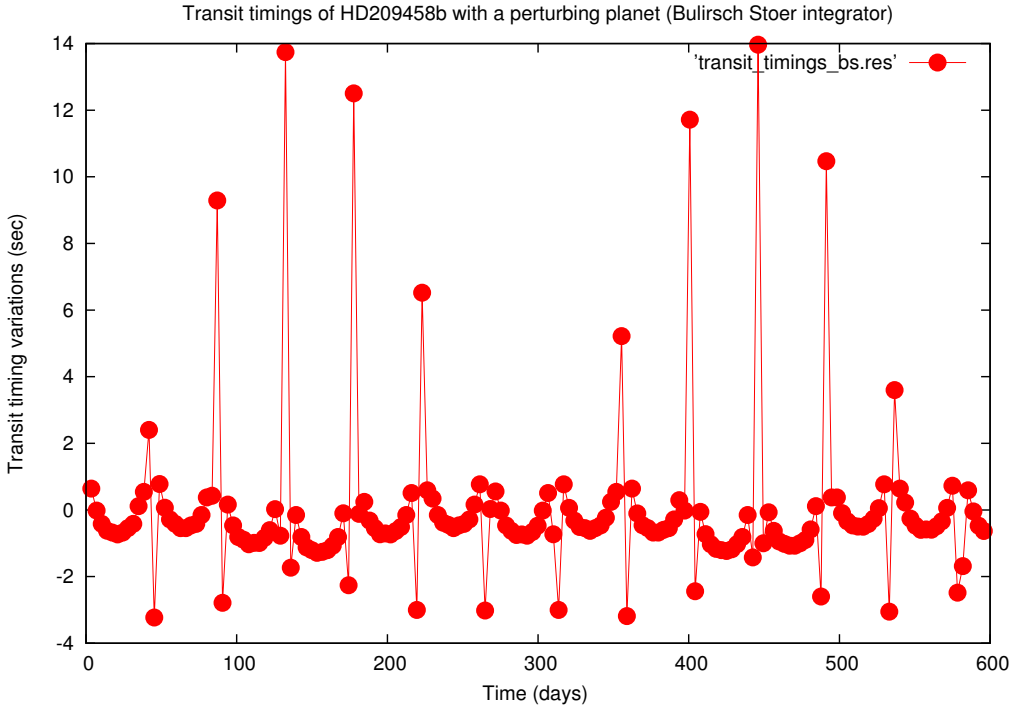

Figure 7: Transit timings computed with the Bulirsch Stoer integrator.

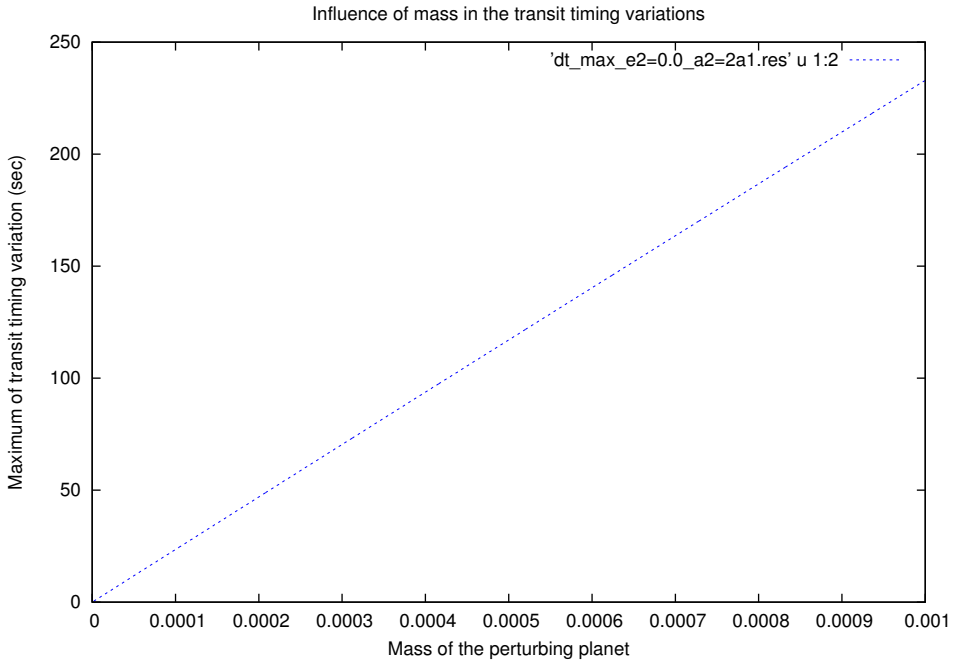

Figure 8: Maximum of timing variation with respect to the perturbing planet mass. $e_2 = 0$ and $a_2 = 2 \times a_1$

Eccentricity: the figure 9 shows us that the eccentricity affect heavily the variations. The eccentricity affects mainly the indirect effect (the motion of the star) because when the perturbing planet reaches its periapse, its velocity is maximum. As a consequence, the star moves faster than usual, thus the variations in the interval between two transits will be maximum when the perturbing planet is close to its periapse.

Argument of periapse: the angle is directly related to the eccentricity. As shown in figure 10 the direction of the effect changes but not its amplitude. And as a result transit can occur late or early, see firgure 11. However, we can also find angles for which the variations will be minimum, as shown in figure 11 in the bottom right .

We will now considerate three different cases.

3.2 Planets on circular orbits

Both planets are on a circular orbit. Immediately:

- Eccentricity, $e_2 = 0$.

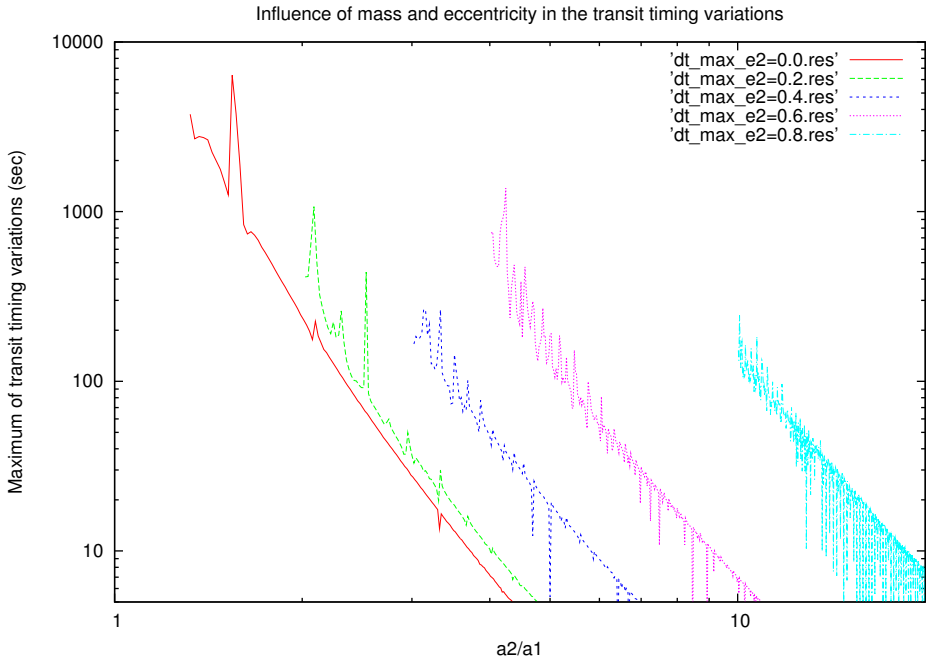

Figure 9: Maximum of timing variation with respect to the perturbing planet semi-major axis. $m_2 = 1 \times 10^{-3} M_\star$ From left to right, eccentricity increases. The peaks are due to the mean motion resonances.

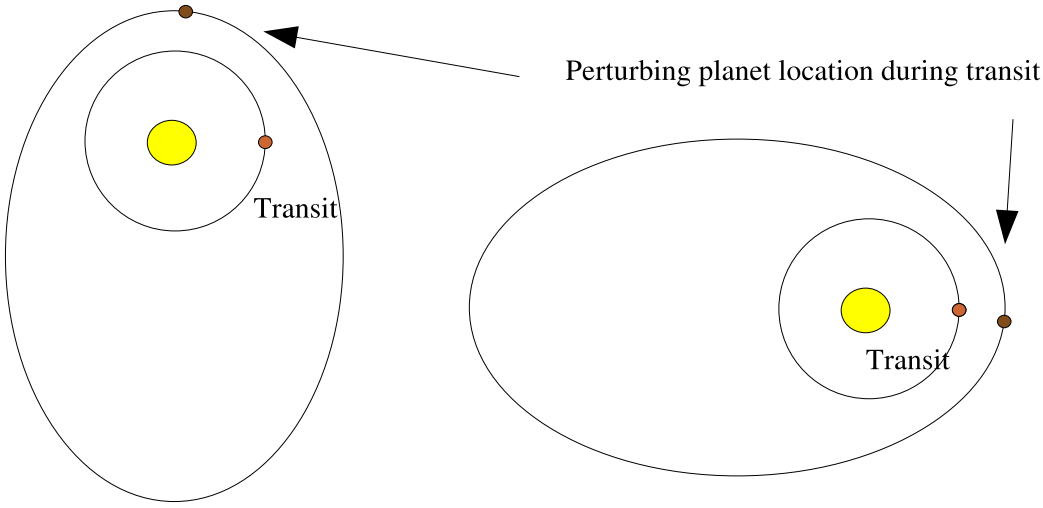

Figure 10: Effect of the argument of periapse. Right: $\varpi_2 = 0$, left: $\varpi_2 = \pi/2$. The figure on the left shows the indirect and direct effects are not symetric anymore.

- Argument of periapse, $\varpi_2 = 0$.
- Mean anomaly (at t = 0), $M_2 = 0$.

Only semi-major axis and mass vary. Figure 12 presents several configurations, all of them are not producing resonances. As seen in figure 9 semi major axis must be inferior to $4 \times a_1$ to allow us to see the variations, taking into account the observational constraints.

3.3 Planets in mean-motion resonance

We are now interessed in the mean motion resonance and we compute transit timings for the 2:1, 3:2, 3:1 and 4:1 resonances. As we saw above, resonances increase the amplitude significantly. This case is very interesting because it allows the detection of very far or small planets.

3.4 Perturbing planet on an eccentric orbit

In this last subsection, we compute four examples where eccentricity goes from 0.1 to 0.7. I took the same idea as N. Murray and M. Holman (2004) proposed: semi-major axis and eccentricity are set to give the same amplitude.

From left to right and top to bottom, period increases. This is also very important, because in this case, the period of the perturbing planet appears directly in the curve. With great eccentricites, this latter can be evaluated

with a very good accuracy. Moreover we get the mean anomaly M_2 (since we see when the perturbing planet reaches its pariapse).

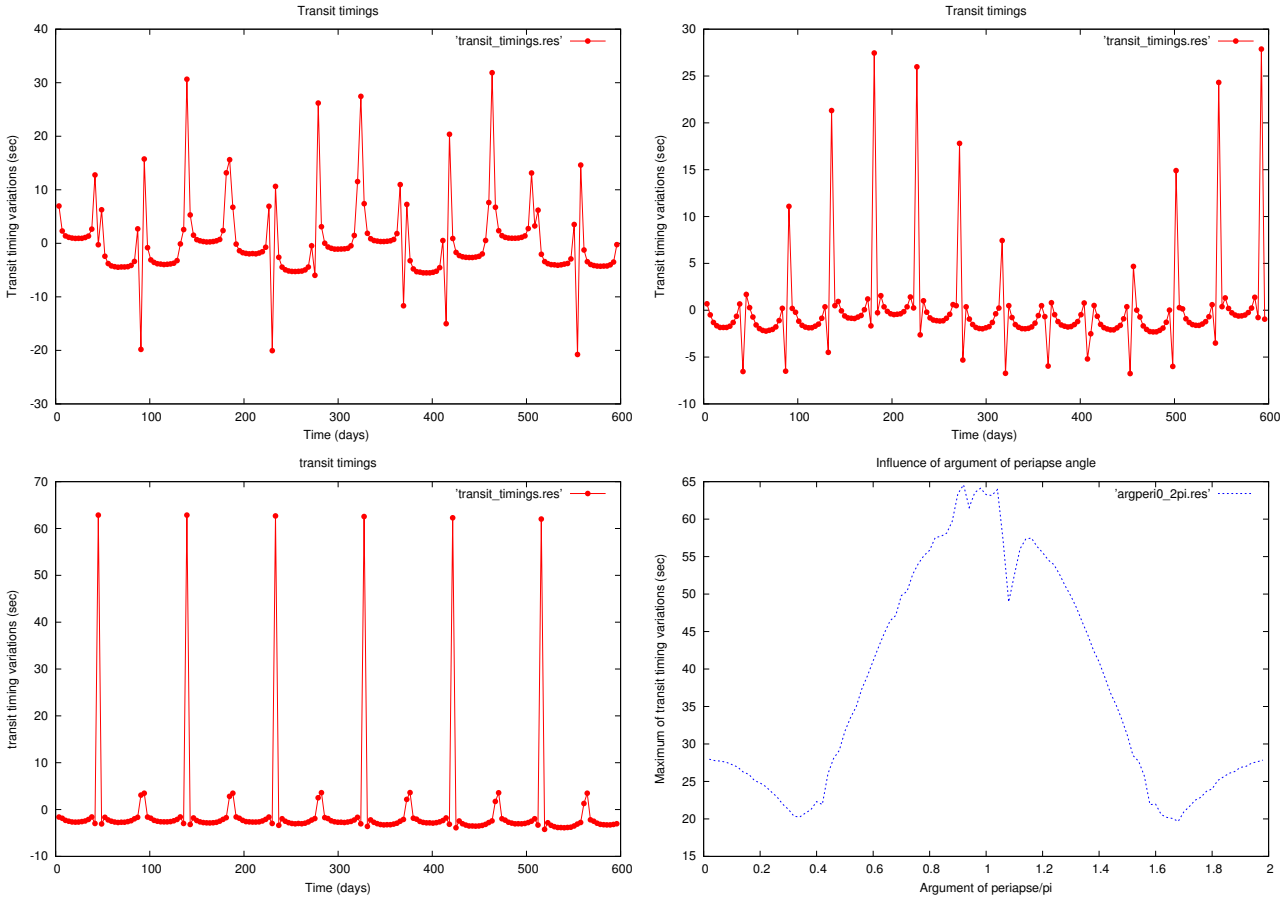

Figure 11: Effect of the argument of periapse. Top left: $\varpi_2 = \pi/2$, top right: $\varpi_2 = 0$, bottom left $\varpi_2 = \pi$. In the figure on the top right, the planets are closer when the perturbing one reaches its periapse, the direct effect (from the perturbing planet) tends to oppose the direct effect. In the figure on the bottom left the planets are the farthest during the transit. Bottom right: maximum of transit timing variations with respect of the argument of periapse angle. When $\varpi = \pi$, the direct effect is negligible compared to the indirect effect.

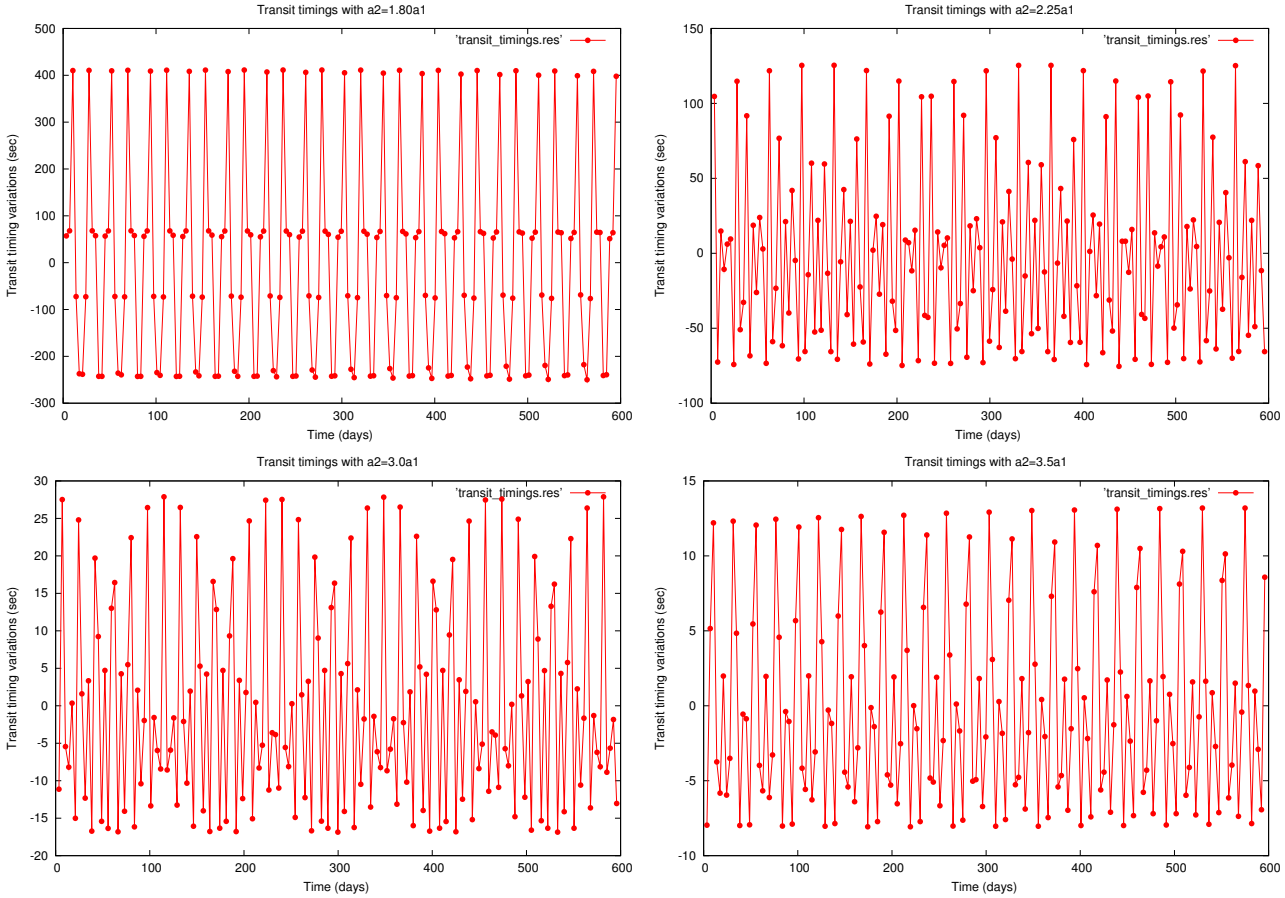

Figure 12: Examples of timing varitions due to a perturbing planet on a circular orbit.

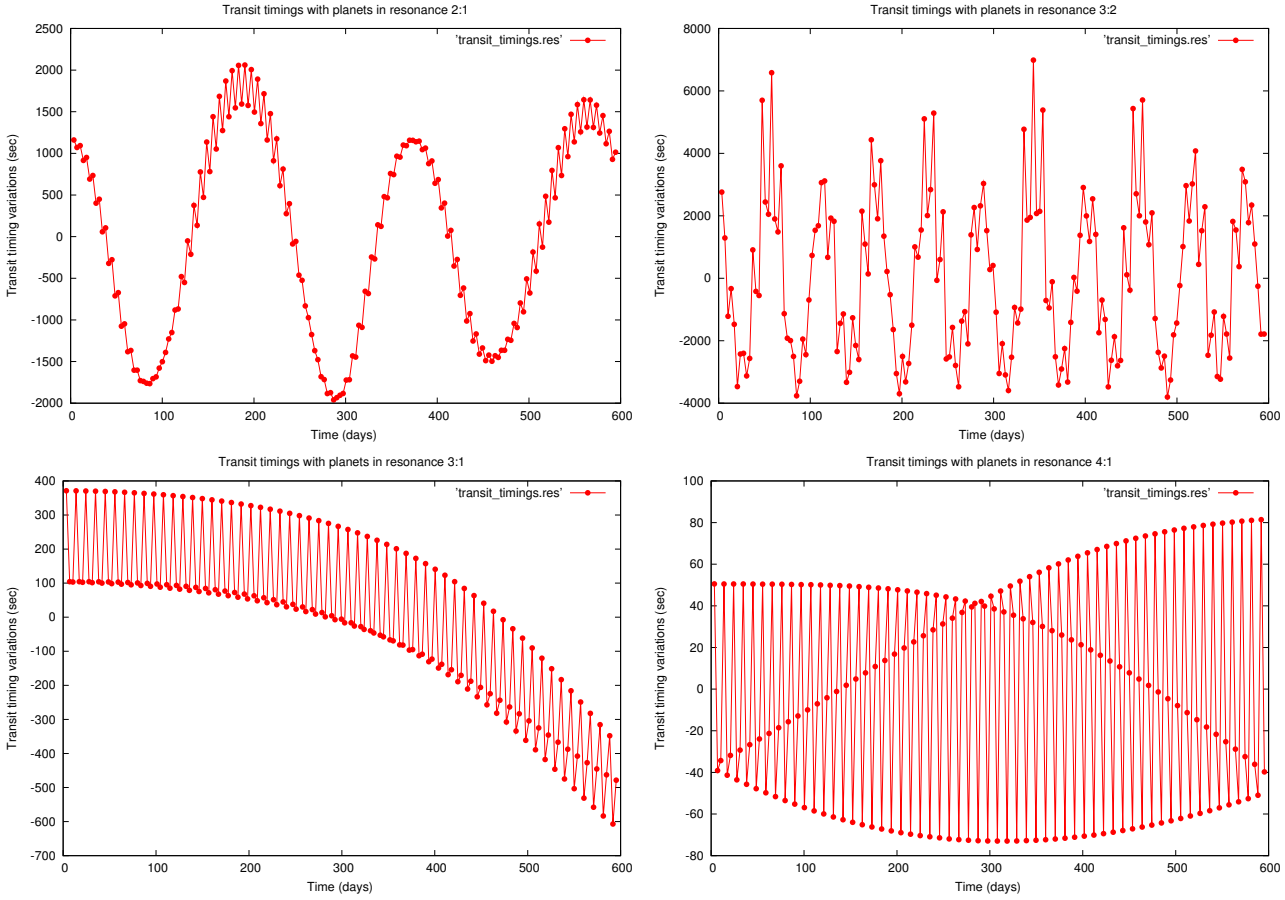

Figure 13: Examples of timing varitions due to planets in resonance.

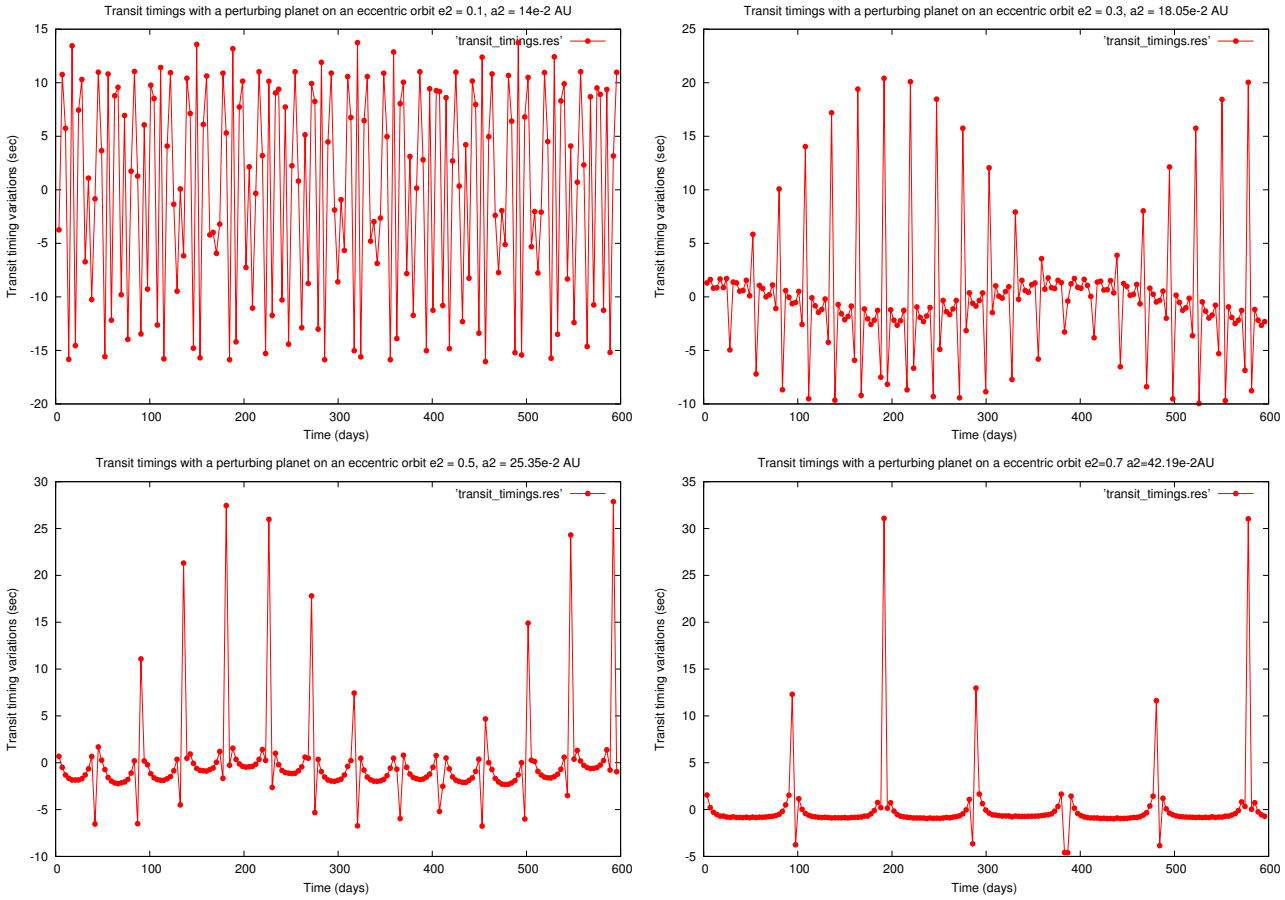

Figure 14: Examples of timing varitions due to a perturbing planet on an eccentric orbit. Top left: $T_2 = 19.2 days$, top right: $T_2 = 27.9 days$, bottom left: $T_2 = 46.6 days$ and bottom right $T_2 = 100.0 days$

Part II
Problem inversion

This part represents the main interest of this project. We will now try to invert the problem. Given a set of transit timings, to invert the problem consists in finding the closest parameters which fit the data. To do so we will use the χ^2 minimization method.

However, before taking numerical aspects into consideration, we must use our first results to draw fisrt conclusions. This way, we will be able to constrain the system we are studying and also prevent errors (because of degeneracies). This is the first subsection.

When it is done, we can finally let the computer do and wait for the results. Before that I will explain how I wrote the code which perform calculations in a second subsection.

At the end we will study the same cases I described in the last section of the previous part.

1 Constraints and degeneracies

1.1 Observable systems and constraints

The condition we must face is the amplitude of the timing transit. Let's recall how parameters change the amplitude of variations.

The maximum of variations is nearly a linear function of mass and a monotone function of semi-major axis (except for resonances). Large eccentricities make possible great variations when the perturbing planet is close to the periapse. And finally, the effect is maximum when direct and indirect effects act in the same direction, i.e. when the argument of periapse equals π.

We assumed a gaussian noise for the data. If we call σ, the standard deviation, the true value of the transit timing variation will be in the range $\pm 3\sigma$ with a probability of 99.7 %. Consequently, if we want to "see" the variations, the perturbing planet must create variations in the transits intervals, bigger than 3σ.

This is our condition to observe two-planet systems:

$$\Delta(t) > 3\sigma \tag{7}$$

As M. Holman and N. Murray showed, one can approximate the amplitude of timing variations by the expression:

$$\Delta(t) \sim \frac{45\pi}{16}\left(\frac{m_2}{M_\odot}\right) T_1 \alpha_e^3 \left(1 - \sqrt{2}\alpha_e^{3/2}\right)^{-2} \tag{8}$$

with

$$\alpha_e = \frac{a_1}{a_2(1-e_2)} \tag{9}$$

This expression underestimates the true values, because it was derived with a parabolic orbit for the perturbing planet. We can notice that for a same period ratio of the two planets, the timing variation increases with the period of the transiting planet.

First constraint: As shown in figure 15, for masses of the perturbing planet below $m_2 = 10^{-5} M_\odot$, observations are difficult.

Second constraint: In the same way, for any eccentricities, $a_2 = 30 a_1$ appears to be an upper limit for observations.

Third constraint: In the numerical computations, we noticed that the argument of periapse can reduce the effect if the perturbing planet reaches its periapse on the same side of the transit location (when the angle equals 0 in our model). We express the constraint in this manner: for small masses ϖ_2 must be close to π.

Fourth constraint: We know resonances can lead to important timing variations. Then we must take this element into account and it represents one of the most interesting point in this study. Thus the third constraint is expressed as follow. If the mass of the perturbing planet is smaller than $m_2 = 10^{-5} M_\odot$, planets must be in resonance in order to observe perturbations. The minimum value allowed for m_2 is now $m_2 = 5.10^{-6} M_\odot$.

One another remarkable fact regarding resonances. Since we know that the effect increases with respect to the period of the transiting planet, we can evaluate the minimum mass required for larger periods of the transiting planet as well.

Figure 16 shows that m_2 can be as small as $m_2 = 2.10^{-6} M_\odot$ for a a bigger period of the transiting planet .

1.2 Simple cases

As we saw, planets in resonance will be easy to study since long term variations can be easily detected. (Especially for first order resonances and m:1 resonances). Let n_2 and n_1 the mean motions of the perturbing planet and the transiting one. If the planets are in resonance:

$$\frac{n_2}{n_1} = \frac{p}{p+q} \tag{10}$$

Where p and q are integers. The conjunction period is given by:

$$T_{conj} = \frac{2\pi}{n_1 - n_2} \tag{11}$$

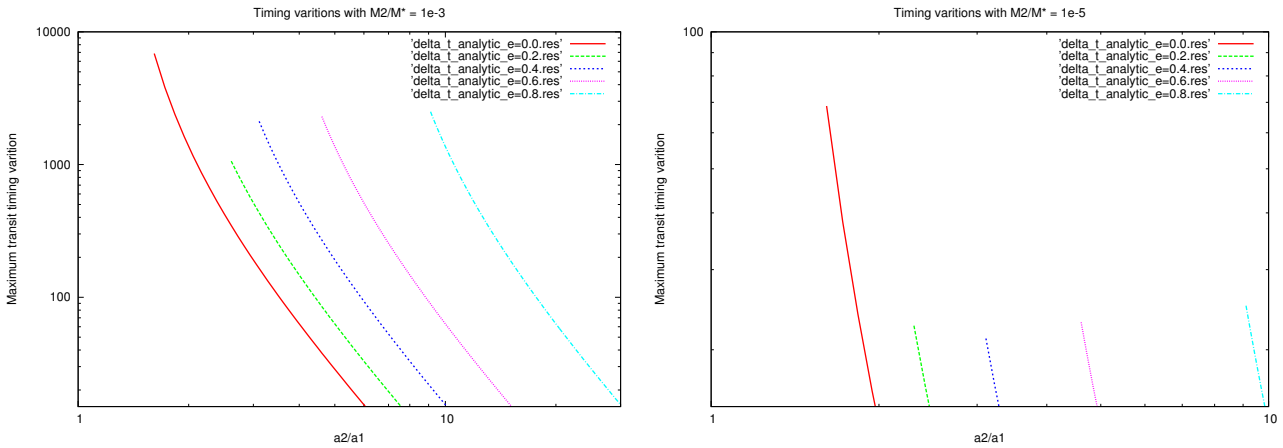

Figure 15: According to expression 8, maximum of the timing transit is computed with respect of the semi-major axis of the perturbing planet for several eccentricities. The minimum is fixed at $3\sigma = 15$ sec. The transiting planet is a HD209458-type planet with $T_1 = 3.58$ days and $a_1 = 4.5 \times 10^{-2}$ AU. The figure on the left shows variations for a perturbing planet with mass $m_2 = 10^{-3} M_\odot$. On the right $m_2 = 10^{-5} M_\odot$.

Let's assume $e1 = 0$ and $e2 = 0$

$$(p+q)n_2 - pn_1 = 0 \tag{12}$$

We can write the resonant argument:

$$\phi = (p+q)\lambda_2 - p\lambda_1 \tag{13}$$

Which represents the frequency of the perturbation (in the first order).
For a 2:1 resonance:

$$\phi_{perturb} = 2\lambda_2 - 1\lambda_1 \tag{14}$$

and

$$T_{perturb} = 2T_1 \tag{15}$$

For a 3:1 resonance:

$$T_{perturb} = 3T_1 \tag{16}$$

The firgure 17 illustrates these results.
The long period variations depend on the eccentricity of the transiting planet, even it is small.

An other simple case occurs when the amplitude is much greater than the noise, where the curve pattern is sufficiently readable (for example $m_2 > 10^{-5} M_\odot$ and $a_2/a_1 < 3$).

Finally, large eccentricities produce very specific timing varitions. In this case we can directly access to the period of the perturbing planet, because large peaks occur only when the latter is near the periapse. In the same way we know the periapse passage time (so the mean anomaly a $t = 0$).

1.3 Degeneracies and critical cases

For one set of parameters there is only one set of timing variations. The critical cases are defined by small timing variations in general, where we cannot distinguish the pattern very well, but only the amplitude. And on the contrary of the pattern case, the maximum amplitude is strongly degenerated.

Unfortunatly, we don't have enough accurate analytic expressions. We can already think that error evaluations will be difficult because of degeneracies.

For a HD209458-type planet with a period $T_1 = 3.58$ days, it is difficult to distinguish the period of the perturbing planet when its eccentricity is below 0.2-0.3.

If the semi-major axis of the perturbing planet is held fixed, there is a strong degeneracy caused by mass and eccentricity (0.0 to 0.3).

Also because of small eccentricities, angles (mean anomaly at $t = 0$ and argument of periapse) will be difficult to find.

Finally, in general, variations of the semi-major axis will imply dramatic changes in the curve pattern. On one hand it is a good point for the inversion, because while we don't have a good guess for the semi-major axis, minimization algorithms will not converge towards a local minimum. On the other hand there is a chance we wait a lot before having a good guess.

2 Minimization

2.1 Data fitting with the χ^2 method

We want to learn more about the orbital elements of the perturbing planet. Therefore data fitting is necessary. Let us suppose we have a data set of transit timings, $\Delta_{data}t(t)$

We use the least square minimization to find estimators of the parameters. The aim is to find a model $\Delta_{model}t(t)$ which minimizes the quantity:

$$\chi^2 = \sum_{i=1}^{N} (\Delta_{data}t(i) - \Delta_{model}t(i))^2 \tag{17}$$

Where N is the number of transits observed and i the i^{th} transit.

I first used a simplex method algotrithm in N-dimensions. But the method was not enough efficient and took a very long time. Then I searched for a better method and found the answer in the gradient method and I used the functions of the Numerical Recipes.

This method is very fast and efficient. The problem is that the algorithm needs to know the derivatives of the function ($\frac{\partial \Delta_{model}}{\partial a_2}$, $\frac{\partial \Delta_{model}}{\partial e_2}$, etc.) to evaluate the slope of the χ^2 (the gradient).

I had to evaluate first the "curvature scale " of the χ^2 with respect to each parameters. Then we can accomplish the numerical derivatives:

$$\frac{\partial \Delta_{model}}{\partial a} = \frac{\Delta_{model}(a+h) + \Delta_{model}(a-h)}{2h} \tag{18}$$

Where $h = (\varepsilon)^{1/3} a_c$. ε is the accuracy with which the function is evaluated, here $\varepsilon \approx 1sec$, and a_c is the curvature scale (which must be estimated for each parameter a).

One call of the routine finds the local minimum. To find the global one, the idea is to draw the parameters and wait until the guesses lead to a good fit.

How to evaluate the goodness of fit? If ν is the degree of freedom of χ^2, a moderately good fit is about $\approx \nu$. And ν equals the number of points - the number of parameters. In our case, $\chi^2 \approx \nu \approx 170$.

To improve the method, we can add some a priori information on our system.

Maximum of the data set: Because of the noise, important degeneracies can occur if the data contains only a few peaks. As a consequence, the χ^2 has several local minima. To avoid this problem, we can eliminate solutions (i.e. parameters set) which cannot produce such peaks.

Semi-major axis: We know with a good accuracy the value of the semi-major axis when the perturbing planet has a large eccentricity. A narrow range can be used for the guesses of a_2.

Eccentricity: On the contrary, if we are not able to extract a value for the semi-major axis, we know that eccentricity must be in the range [0.0:0.3].

Stability of the system: A simple condition for the stability of the system is that planets must be out their mutual spheres of influence (Roche zone, R_1, R_2) to avoid close encounters:

$$a_1(1+e_1) < (R_2+R_1)a_2(1-e_2) \tag{19}$$

Signs: And finally, all parameters must be positive.

2.2 Uncertainties and confidence limits

The covariance matrix is directly given by the routine of Numerical recipes. Since we are in the gaussian case for noise we can write:

$$\Delta\chi^2 = \delta\mathbf{a} \cdot [\alpha] \cdot \delta\mathbf{a} \tag{20}$$

Where $\delta\mathbf{a}$ is the parameter vector and $[\alpha]$ is the inverse of the covariance matrix. $\Delta\chi^2$ is defined by:

$$Q(\nu/2, \Delta\chi^2/2) = \frac{\Gamma((\nu/2, \Delta\chi^2/)}{\Gamma(\nu/2)} = 1 - p \tag{21}$$

Where Q is the incomplete gamma function and p the confidence level (%). ν is the degree of freedom (here, the number of parameters). For example if we want the confidence intervals for two parameters, $\nu = 2$ and for p = 99.73 %, $\Delta\chi^2 = 9.00$;
At the end, equation (20) gives the equation of an ellipse.

2.3 Accuracy and computation times

With the gradient method, the minimization code gives the best estimation for the local minima. For example, without noise, it converges very rapidly to $\chi^2 = 0.1 - 0.01$ Then we can expect that the minimum, with noise, is also given with a very good accuracy. The errors are mainly due to the noise and we know how to estimate the confidence intervals.

It takes about 3 seconds to compute a set of transit timings (170 transits) with a "regular computer". As seen in the equation (18) for the derivatives, we need to compute the transit timing function two times for each parameter (and one time for the value of $\Delta_{model}(\mathbf{a})$). If we want to estimate the 5 parameters (m_2, a_2, e_2, ϖ_2 and M_2), it takes $5 \times 3 \times 3 = 45$ sec a step. In general, the code needs about 20 steps to reach a minimum, so 15 minutes. At the end, we can expect to have a global minimum in a reasonable time of computation (a few hours).

3 Results

In this section, I present a few examples to illustrate this part. All of these calculations have been made with 30 transits. For the fourth first subsections, angles (ϖ, M_2) are set to zero and non evaluated.

The last subsection presents a result with all the parameters and 170 transits.

3.1 χ^2 surfaces

First, let us have a look at the χ^2 surfaces. All of them are plotted without noise, then the global minimum is zero.

Figure 18: shows the χ^2 surface with respect to e_2 and m_2. Here we can see there's only one minimum and the surface is very smooth. We can expect no difficulties to find the minimum in this case. However, once we introduce noise, degeneracies near the minimum will give many set of values for e_2 and m_2.

Figure 19: shows the χ^2 surface with respect to e_2 and a_2. Here we can see several local minima. Either we will need a first estimation for a_2, either we will need to draw random values and wait for the global minimum to be found. What we can also notice is the other minima have much higher values of χ^2 than the global one, which is very usefull to say if we found the good ranges of parameters or not.

Figure 20: shows the χ^2 surface with respect to a_2 and m_2. We can draw the same conclusion than the previous case, except that, as we already know, mass variations are almost linear, and minima in this case are found very fast.

Once the semi-major is found, the other parameters are easy to find. This fact confirms what we found above: the semi-major axis changes strongly the shape of the transit timing set. As a conclusion, we can say that the semi-major axis will be find with a good accuracy, however, degeneracies will occur between mass and eccentricities.

All the followings results have been computed with a HD209458b-type planet with the parameters:
Mass, $m_1 = 10^{-3} M_\odot$
Semi-major axis, $a_1 = 4.5 \times 10^{-2} AU$
Eccentricity, $e_1 = 0.025$
Argument du periapse, $\varpi_1 = 0$
Mean anomaly, $M_1 = 0$

We assumed a gaussian noise with $\sigma = 5$ seconds and we give the true parameters of the perturbing planet, the estimated parameters, the errors and the covariance matrix.

3.2 Planets on circular orbits

Both planets are on circular orbits. We compute 30 transits and we do not estimate angles.
The true parameters of the perturbing planet are:
Mass, $m_2 = 10^{-3} M_\odot$
Semi-major axis, $a_2 = 8.0 \times 10^{-2} AU$
Eccentricity, $e_2 = 0.0$
Argument du periapse, $\varpi_2 = 0$
Mean anomaly, $M_2 = 0$

The χ^2 minimization gives the following estimators (for $\chi^2 = 27.23$):
$m_2 = 9.942 \times 10^{-2} M_\odot$, e = 0.6 %
$a_2 = 7.999 \times 10^{-2} AU$, e = 0.0125 %
$e_2 = -0.000544$, e = 0.06 %

And the program returns the covariance matrix:

$$[C] = \begin{pmatrix} 3.342 \times 10^{-11} & -4.319 \times 10^{-12} & 3.259 \times 10^{-09} \\ -4.319 \times 10^{-12} & 1.066 \times 10^{-11} & -8.932 \times 10^{-10} \\ 3.259 \times 10^{-09} & -8.932 \times 10^{-10} & 6.979 \times 10^{-07} \end{pmatrix}$$

3.3 Planets in mean-motion resonance

The planets are in the 3:1 resonance. We compute 30 transits and we do not estimate angles.
The true parameters of the perturbing planet are:
Mass, $m_2 = 10^{-4} M_\odot$
Semi-major axis, $a_2 = 9.4 \times 10^{-2} AU$
Eccentricity, $e_2 = 0.0$
Argument du periapse, $\varpi_2 = 0$
Mean anomaly, $M_2 = 0$

The χ^2 minimization gives the following estimators (for $\chi^2 = 28.62$):
$m_2 = 9.752 \times 10^{-5} M_\odot$, e = 2.5 %
$a_2 = 9.404 \times 10^{-2} AU$, e = 0.05 %
$e_2 = -0.01705$, e = 1 %

And the program returns the covariance matrix:

$$[C] = \begin{pmatrix} 1.079 \times 10^{-09} & 2.381 \times 10^{-09} & 2.079 \times 10^{-06} \\ 2.381 \times 10^{-09} & 2.389 \times 10^{-08} & 4.745 \times 10^{-06} \\ 2.079 \times 10^{-06} & 4.745 \times 10^{-06} & 4.201 \times 10^{-03} \end{pmatrix}$$

3.4 Perturbing planet on an eccentric orbit

The perturbing planet is on an eccentric orbit. We compute 30 transits and we do not estimate angles.
The true parameters of the perturbing planet are:
Mass, $m_2 = 10^{-3} M_\odot$
Semi-major axis, $a_2 = 20.0 \times 10^{-2} AU$
Eccentricity, $e_2 = 0.5$
Argument du periapse, $\varpi_2 = 0$
Mean anomaly, $M_2 = 0$

The χ^2 minimization gives the following estimators (for $\chi^2 = 17.42$):
$m_2 = 1.059 \times 10^{-3} M_\odot$, e = 6 %
$a_2 = 0.1999 \times 10^{-2} AU$, e = 0.05 %
$e_2 = 0.4931$, e = 1.4 %

And the program returns the covariance matrix:

$$[C] = \begin{pmatrix} 1.019 \times 10^{-08} & -2.224 \times 10^{-09} & -5.972 \times 10^{-07} \\ -2.224 \times 10^{-09} & 7.378 \times 10^{-09} & 3.556 \times 10^{-07} \\ -5.972 \times 10^{-07} & 3.556 \times 10^{-07} & 5.778 \times 10^{-05} \end{pmatrix}$$

3.5 Estimation of all parameters

We now include the angles (argument of periapse and mean anomaly) in the estimation. We compute 170 transits with a perturbing planet and we assume a narrow range for the semi-major axis and also for the mean anomaly.

The true parameters of the perturbing planet are:
Mass, $m_2 = 10^{-3} M_\odot$
Semi-major axis, $a_2 = 25.35 \times 10^{-2} AU$
Eccentricity, $e_2 = 0.5$
Argument du periapse, $\varpi_2 = 0$
Mean anomaly, $M_2 = 0$

The χ^2 minimization gives the following estimators (for $\chi^2 = 160.74$):
$m_2 = 9.269 \times 10^{-4} M_\odot$, e = 7.4 %
$a_2 = 25.347 \times 10^{-2} AU$, e = 0.02 %
$e_2 = 0.4978$, e = 0.5 %
$\varpi_2 = 0.2389$, e = 24 %
$M_2 = -0.02772$, e = 3 %

And the program returns the covariance matrix:

$$[C] = \begin{pmatrix} 8.383 \times 10^{-09} & -1.995 \times 10^{-09} & -4.026 \times 10^{-07} & 1.4504 \times 10^{-06} & -1.504 \times 10^{-07} \\ -1.995 \times 10^{-09} & 1.6953 \times 10^{-08} & 1.250 \times 10^{-07} & 1.776 \times 10^{-06} & 1.776 \times 10^{-06} \\ -4.026 \times 10^{-07} & 2.250 \times 10^{-07} & 7.953 \times 10^{-05} & 1.9328 \times 10^{-04} & -1.647 \times 10^{-04} \\ 1.4504 \times 10^{-06} & 3.877 \times 10^{-06} & 1.932 \times 10^{-04} & 1.621 \times 10^{-02} & -3.823 \times 10^{-03} \\ -1.504 \times 10^{-07} & 1.7758 \times 10^{-06} & -1.647 \times 10^{-04} & -3.823 \times 10^{-03} & 1.738 \times 10^{-03} \end{pmatrix}$$

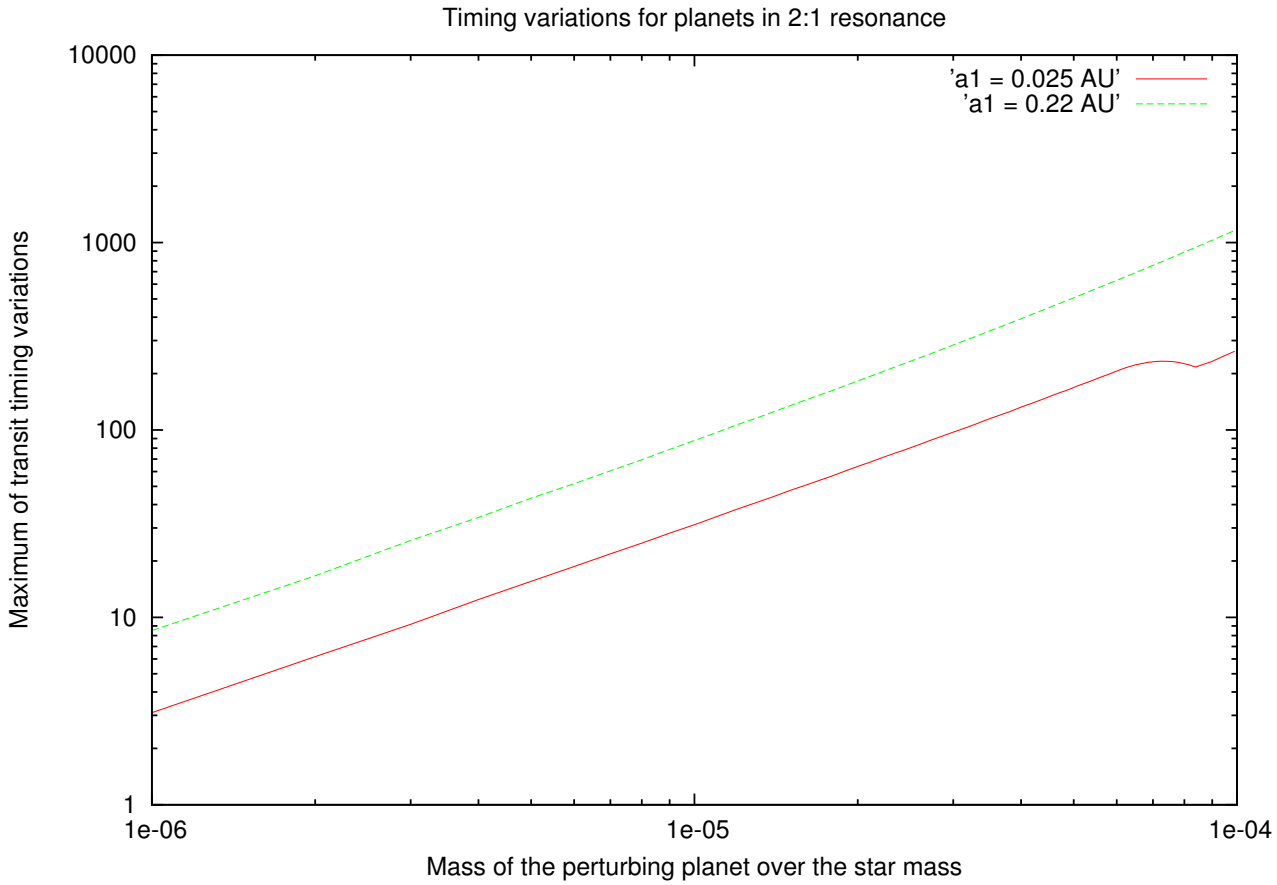

Figure 16: Numerical computations to determine minimum masses allowed for planets in a 2:1 mean-motion resonance. The lower curve corresponds to a HD209458b-type planet, the minimum mass we are able to detect is $m_2 = 5.10^{-6} M_\odot$. The upper curve corresponds to a rho-CrBb-type planet, the minimum mass in this case is $m_2 = 2.10^{-6} M_\odot < M_\oplus$ (But observations must be longer).

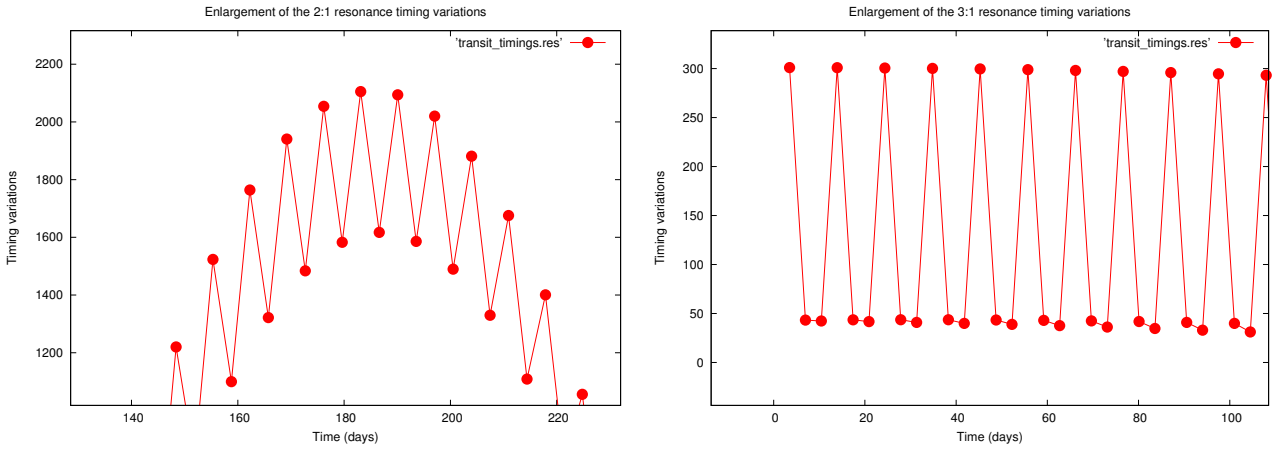

Figure 17: Enlargement of the transit timing variations due to planets in 2:1 (left) and 3:1 (right) resonnances. A first look at the varations allow us to determine the resonance order.

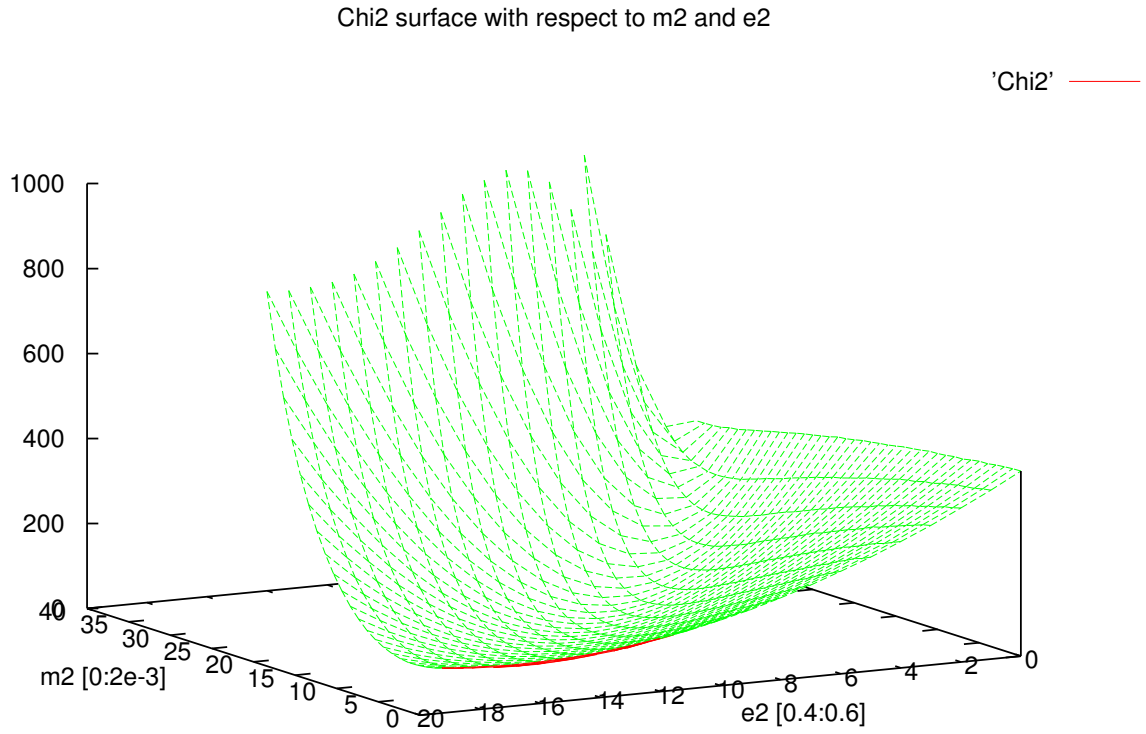

Figure 18: χ^2 surface when m_2 and e_2 vary (arbitrary units). All other parameters are held fixed. The global minimum is easy to reach.

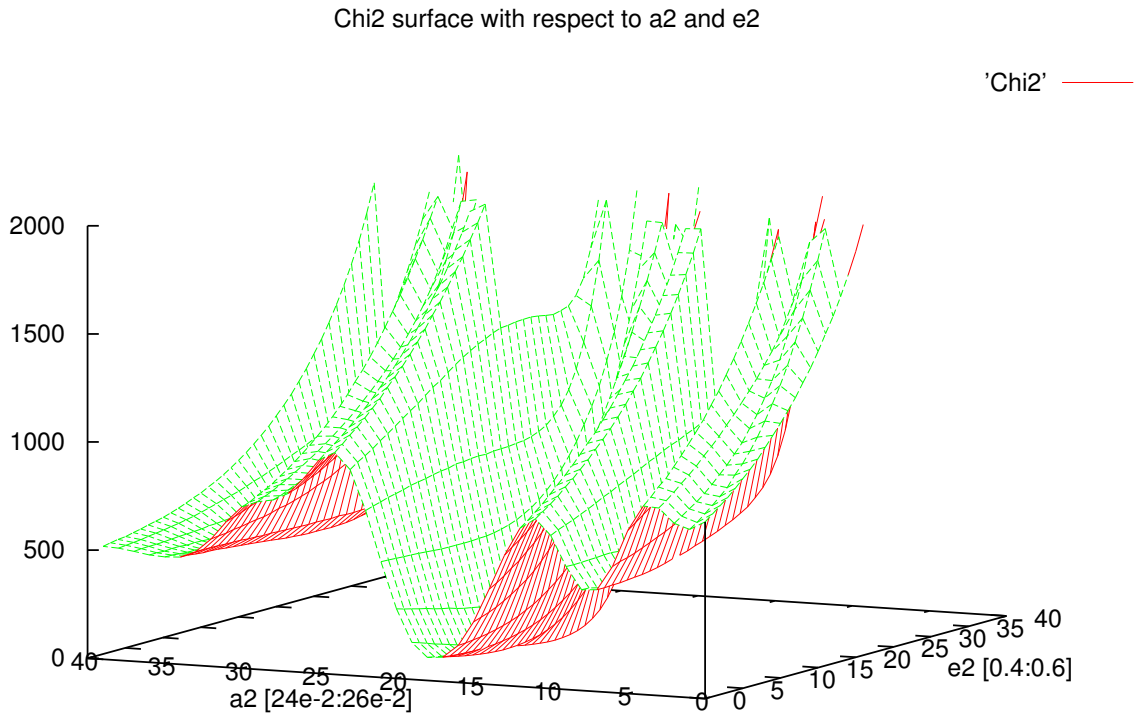

Figure 19: χ^2 surface when a_2 and e_2 vary (arbitrary units). All other parameters are held fixed. The global minimum is located in the middle of the figure. As soon as a good (and narrow) range for a_2 is given, the global minimum can be found easily

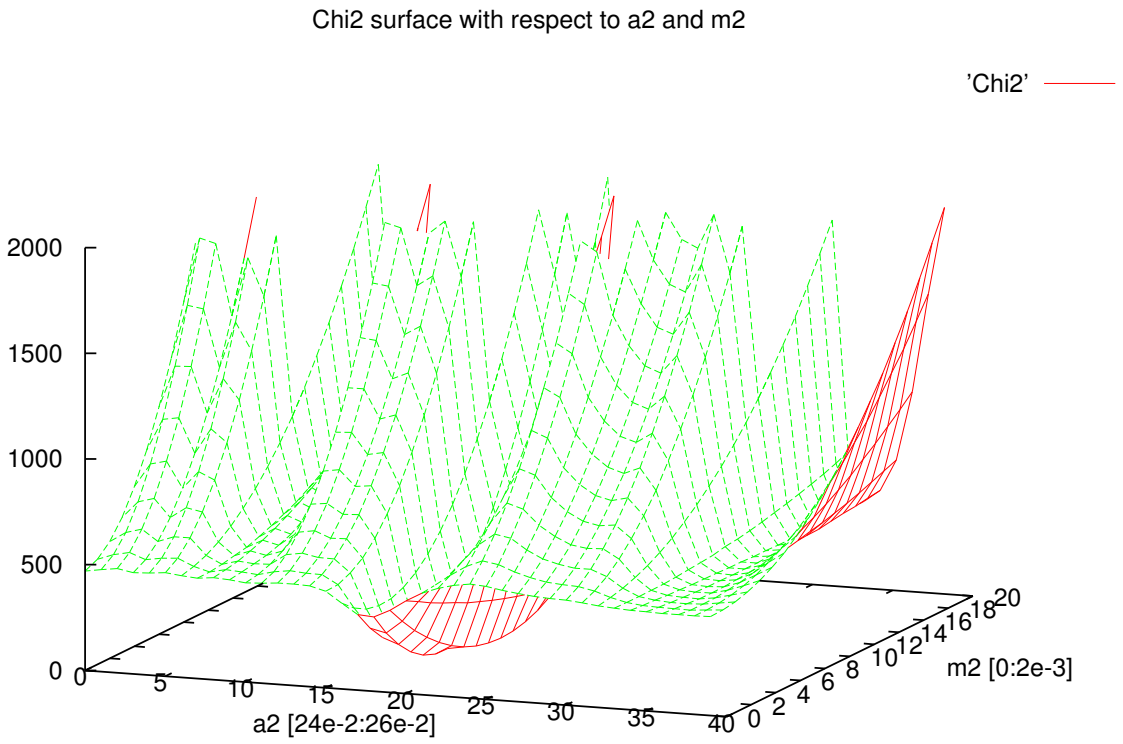

Figure 20: χ^2 surface when a_2 and m_2 vary (arbitrary units). All other parameters are held fixed. The global minimum is located in the middle of the figure. Same remark than for the previous figure, we need a good estimation for a_2

Conclusion

We learnt from the first part how a second planet in a system could lead to perturbations on a transiting planet. The most important points were to understand the effects on the transit timings and the dependencies of the parameters.

The transit timing variations are linearly depend to the mass, exept for the resonances and very close planets (where perturbations due to the transiting planet on the second planet cannot been neglected anymore).

Newtonian motions of the planets can be approximated since other perturbations (tides, general relativity, etc.) induce only secular perturbations.

The numerical results showed us the transit timing variations in three different cases: for planets on circular orbits, in mean-motion resonances and for a perturbing planet on an eccentric orbit. The two last cases are easier to observe and allow a direct estimation for some orbital elements of the perturbing planet (such as the semi-major axis and the periapse time passage).

In the second part, we answered our question of how to find the parameters of a perturbing planet.

Observable systems are constrained by the orbital elements of the planets. If we are looking at a HD209458b-type transiting planet, mass of the outer planet must be greater than $10^{-5}M_{\odot}$, except if the planets are in resonance, then we can detect planets down to $5 \times 10^{-6}M_{\odot}$ ($\approx M_{\oplus}$)!.

The semi-major axis of the outer planet must be less than 30 times the semi-major axis of the inner planet (with an eccentricity of 0.8 and a mass of $10^{-3}M_{\odot}$). For most cases, perturbing planets will be detected in the range $1.5a_1$ to $4a_1$.

As we saw in the last subsection, the χ^2 minimization works well. However at this stage we neglected a lot of things. For example, the angles will be probably difficult to estimate and lead to degeneracies with the other parameters. Also, we assumed coplanar orbits. This assumption is good for planets in circular orbits since the interactions between them will reduce inclination. But if the perturbing planet is on a large eccentric orbit (with a long semi-major axis), the assumption is obviously wrong.

Nevertheless, the method works. We also proved we cannot have degeneracies of completly different systems and once we have a set of parameters, the true ones are within the confidence intervals.

Regarding my work. When Norm Murray and Mat Holman wrote their paper, they proved that a new method to detect extrasolar planets was doable. I tried to go further in order to know how to realize such a study. Unfortunatly, data are not available yet and I regret not to have been able to confront my work to hypothetical ones. Moreover, I wish I had more time to go more in-depth in the analytical study of this problem. I was very excited by this subject and I appreciated to spend these three months at the Canadian Institute for Theoretical Astrophysics which is a very lively place.

Acknowledgments

I thanks Norm Murray and Yanqin Wu who helped me to do this project. I also thanks Marc Goodman and the staff of the Canadian Institute for theoretical Astrophysics. I would like to thank all the graduate students and especially Alexandre Bouquin who has helped to review this report.

Finally, thanks to the people in charge of the Master Astronomie et Astrophysique and all my professors I had this year.

References

[1] M. J. Holman, N. W. Murray (2004). *Science* **307** (2005).

[2] E. Agol, J. Steffen (2005). *Mon. Not. R. Astron. Soc.* **364** (2005).

[3] E. Agol, J. Steffen (2005). *Mon. Not. R. Astron. Soc.* **359** (2005).

[4] Numerical Recipes in C.

[5] D. Pelat (2005). Cours de bruits et signaux.

[6] B. Sicardi (2005). Resonances et marees dans le systeme solaire et les disques.

[7] J. Schneider (2004). http://www.obspm.fr/encycl/catalog.html.

[8] I. A. Bond, *et al.*, *ApJ* **606**, L155 (2004).

[9] A. Wolszczan, D. A. Frail, *Nature* **355**, 145 (1992).

[10] D. C. Backer, R. S. Foster, S. Sallmen, *Nature* **365**, 817 (1993).

[11] M. Mayor, D. Queloz, *Nature* **378**, 355 (1995).

[12] G. W. Marcy, R. P. Butler, *ApJ* **464**, L147+ (1996).

[13] D. Charbonneau, T. M. Brown, D. W. Latham, M. Mayor, *ApJ* **529**, L45 (2000).

[14] G. W. Henry, G. W. Marcy, R. P. Butler, S. S. Vogt, *ApJ* **529**, L41 (2000).

[15] A. Udalski, *et al.*, *Acta Astronomica* **52**, 1 (2002).

[16] A. Udalski, *et al.*, *Acta Astronomica* **52**, 115 (2002).

[17] A. Udalski, *et al.*, *Acta Astronomica* **53**, 133 (2003).

[18] B. E. McArthur, *et al.*, *ApJ* **614**, L81 (2004).

[19] P. Butler, *et al.*, *ArXiv Astrophysics e-prints* (2004).

[20] R. Narayan, A. Cumming, D. N. C. Lin, *ArXiv Astrophysics e-prints* (2004).

[21] E. W. Brown, *MNRAS* **97**, 62 (1936).

[22] S. Soderhjelm, *Astron. Astroph.* **42**, 229 (1975).

[23] P. Bodenheimer, G. Laughlin, D. N. C. Lin, *ApJ* **592**, 555 (2003).

[24] J. Stoer, R. Bulirsch, *Introduction to Numerical Analysis* (New York: Springer-Verlag, 1980).

[25] T. R. Quinn, S. Tremaine, M. Duncan, *AJ* **101**, 2287 (1991).

[26] R. W. Hilditch, *An Introduction to Close Binary Stars* (An Introduction to Close Binary Stars, by R.W. Hilditch. Cambridge University Press, 2001, 392 pp., 2001).

[27] C. D. Murray, S. F. Dermott, *Solar System Dynamics* (Cambridge: University Press, |c1999, 1999).

[28] J. Wisdom, *AJ* **85**, 1122 (1980).

[29] G. Laughlin, J. E. Chambers, *ApJ* **551**, L109 (2001).

[30] G. Laughlin (2004). http://www.transitsearch.org.

[31] J. E. Chambers, G. W. Wetherill, *Icarus* **136**, 304 (1998).

[32] E. Kokubo, S. Ida, *Icarus* **131**, 171 (1998).

[33] J. F. Kasting, D. P. Whitmire, R. T. Reynolds, *Icarus* **101**, 108 (1993).

[34] J. Miralda-Escudé, *ApJ* **564**, 1019 (2002).

[35] D. D. Sasselov, *ApJ* **596**, 1327 (2003).